Surface Investigation, 2001, Vol. 16, pp. 1127–1134
Reprints available directly from the publisher
Photocopying permitted by license only

Quantitative Methods of Restoration of True Topographical Properties of the Objects by Measurement of AFM-Images. 1. Contact Deformations of the Probe and the Specimen

M. O. Gallyamov and I. V. Yaminsky
M. V. Lomonosov Moscow State University, Moscow, Russia

Received 29 November, 1999

Assuming that the height of the objects of the AFM investigation is underestimated because of contact deformations and solving the Hertz contact problem, the general numerical solution of the problem has been obtained. Approximate analytical solutions which are valid for certain relations between the contact geometry parameters have been found for the case of a cylindrical specimen. The solutions obtained agree well with the experimental results. The approach developed made it possible to determine the elastic parameters of an individual microobject adsorbed on the surface of a solid substrate.

INTRODUCTION

Despite the opportunity of achieving a high spatial resolution, information obtained by the probe microscopy methods, in particular, atomic force microscopy (AFM), does not adequately reflect the real peculiarities of the surface in some cases. This is due to artifacts of the method, which are caused by the effect of the investigation instrument on the subjects under study. As a rule, these artifacts can be easily taken into account in the interpretation of AFM results at the qualitative level. However, the specific character of some problems can necessitate quantitative estimates and methods of the restoration of the real structure of the objects.

We analyzed two basic artifacts of AFM, the influence of which is especially important in conducting investigations of individual microobjects adsorbed on the surface of a solid substrate: the effect of the profile broadening [1] and the effect of underestimation of the height of the AFM-images of the objects investigated. The consideration of the latter effect from the viewpoint of the analysis of contact deformations of the probe and specimen is reported below.

CONTACT DEFORMATIONS

Starting with the first works on the AFM-visualization of nucleic acid molecules [2], it has been noted that the heights of the AFM-images of DNA were essentially underestimated as compared to the existing model concepts on the molecule structure. At the same time, the effect of the height underestimate did not clearly manifest itself in some other objects (with similar physical properties but different curvature radii). For example, it was found in the visualization of the virus particles of tobacco mosaic (VTM) and of molecules of the virus RNA [3, 4] that the effect of the height underestimate is inessential for the virus particles. At the same time, the height of the AFM-images of RNA is lowered by more than 50%, in spite of the fact that the objects were, as a rule, visualized on the same picture and at the same scanning force. An application of the method presented below allowed us to describe this effect in a qualitative manner and relate it to the difference between the radii of VTM particles (~10 nm) and particles of nucleic acids (<1 nm).

Following [5], we assumed that the effect of underestimate of the AFM-image heights is related to the contact deformations. Indeed, in the scanning process, the probe and the specimen interact with the forces of the order of $(1-100)\times10^{-9}$ N. It turns out that the contact pressure can comprise a considerable value and lead to contact deformations due to the small value of the curvature radius of the probe nib (~10 nm).

CONTACT OF TWO BODIES

The problem of the contact deformations of two bodies was for the first time solved by H. Hertz [6]. We will base ourselves on this solution [7]. If two contacting bodies are compressed with some force F, they will deform and approach at a certain distance h to each other. Herewith, the contacting region will no longer be a point but a section with a finite area S.

The analysis of the problem includes the consideration of the total curvature tensor of the contacting surfaces $\chi_{\alpha\beta}+\chi'_{\alpha\beta}$. The principle values A and B of the tensor can be expressed through the principal curvature radii of the contacting surfaces. The corresponding formulae are given in [7] for the general case.

The solution of the contact problem, providing that the deformations are small as compared to the corresponding curvature radii, shows that the shape of the contact region is an ellipse with the semi-axes a and b. It permits one to express these values and the value of the approach h caused by the deformation through the known parameters of the problem, the value of the compressing force F, the contact geometry parameters A and B, and the coefficient D, inverse to the effective elastic modulus:

$$D = \frac{3}{4}\left(\frac{1-\sigma^2}{E} + \frac{1-\sigma'^2}{E'}\right), \tag{1}$$

Here E, E', σ and σ' are the Young and the Poisson moduli of the materials of the probe and specimen.

However, as the ultimate formulae expressing the solution of the contact problem represent a system of nonlinear equations with implicit dependences on the unknown parameters a and b [7], either a numerical solution or an additional analysis with simplifying assumptions is necessary for interpreting the experimental results. Below, we will consider the application of the Hertz solution to the analysis of particular cases, which are important for applied problems.

CONTACT OF A SPHERICAL PROBE WITH A SPHERICAL (OR FLAT) SPECIMEN

The problem to be analyzed is topical in the consideration of the contact deformations which appear in scanning of either microobjects with the shape, which can be approximated by a sphere (for example, molecules of a family of proteins and others), or flat specimens, for example, thin films.

If the probe and the specimen are described by spherical surfaces near the contact point and characterized by the curvature radii R and R', then

$$A = B = \frac{1}{2}\left(\frac{1}{R} + \frac{1}{R'}\right).$$

It follows that $a = b$ and the relations between the parameters of the problem become substantially simplified. One can easily show that the contact region will represent a circle with the radius a:

$$a = (FD)^{1/3}\left(\frac{1}{R} + \frac{1}{R'}\right)^{-1/3}. \tag{2}$$

The following formula is valid for the value h in this case:

$$h = (FD)^{2/3}\left(\frac{1}{R} + \frac{1}{R'}\right)^{1/3}. \tag{3}$$

The formulae (2), (3) are used, for example, by the authors of [5], for model estimates, which are extremely important for an adequate interpretation of the results of AFM investigations (especially, investigations of bipolymers which are characterized by a sufficiently low Young's modulus: $E \sim 10^8 - 10^{10}$ Pa).

However, the formulae indicated are a consequence of the solution of the contact problem for a particular case and are inapplicable, for example, to the analysis of contact deformations of the probe and cylindrical specimen.

CONTACT BETWEEN A SPHERICAL PROBE AND CYLINDRICAL SPECIMEN

The model of a cylindrical specimen should be considered in the analysis of deformations (in AFM studies) of cylinder-shaped micro-particles (virus particles, various linear macromolecules and so on).

In the case when a spherical probe with the radius R contacts with the lateral surface of a cylinder (specimen) of the radius R', the parameters A and B are expressed as follows:

$$A = \frac{1}{2}\left(\frac{1}{R} + \frac{1}{R'}\right), \quad B = \frac{1}{2R}. \tag{4}$$

However, the relations representing a solution of the contact problem in this case are not directly simplified. The numerical solution is possible but requires preliminary analytical calculations because of the complexity of the system to be solved. Therefore we additionally simplified the initial relations and obtained analytical formulae for two particular cases (close values and different values of the parameters A and B), which can be useful for making estimates in the interpretation of experimental results. Comparison of these solutions to the total numerical solution showed a good agreement (when fulfilling the corresponding conditions of approaches).

The case of different principal values of the summary tensor of curvature of the contacting surfaces. Providing that the cylinder radius is less than that of the probe in the case of a contact between the probe and the lateral surface of the cylinder, the formula (4) indicates that the principal values of the summary tensor of the surface curvature are different: $A > B$. Using the general solution of the contact problem, one can show that $a < b$ in this case. In the case, when this difference is large enough, we can simplify the initial nonlinear integral relations [7] using the asymptotic of the total elliptical integral. The latter is valid providing that $a^2 \ll b^2$, which is not a rigid condition:

$$K(k) = \ln\left(\frac{4}{k'}\right) + \dots, \tag{5}$$

with $k' = \sqrt{1 - k^2}$.

Then, the approach caused by deformation will be

$$h = \left(\frac{4}{\pi^2 C}\right)^{1/3} (C + 1)(FD)^{2/3} B^{1/3}. \tag{6}$$

The structure of this formula coincides with that of the formula (3) for the spherical case.

Here, the dimensionless parameter C depends on the ratio of the parameters a and b of the ellipse:

$$C = \ln\left(\frac{4b}{a}\right) - 1 = \frac{Bb^2}{Aa^2}. \tag{7}$$

Using the equation (7) and the known value of the B/A ratio, one can numerically determine the ratio b/a and, correspondingly, the value of the dimensionless parameter C. The numerical solution shows that the value of the parameter C lies within the range 1–3 for many problems. In particular, one can use the relation $C \approx 2$ with a rather good precision in the analysis of the contact between the probe ($R = 10$ nm) and the molecule of the nucleic acid ($R' = 1$ nm).

The formulae obtained for the parameters a and b of the elliptical region of the contact are somewhat awkward; therefore, we do not present them. Their structure coincides with the structure of the equation (2), though. Thus, all the unknown parameters can be directly expressed through the known quantities (F, D, A, B) and the parameter C, which can be determined from the relation (7) or taken approximately $C \approx 2$.

The case of the close principal values of the summary curvature tensor of the contacting surfaces. The case of the close values A and B is realized, for example, in the problem of the contact between the spherical probe and the lateral surface of the cylinder, providing that the cylinder radius is much larger than the probe radius. Then, according to the relations (4), A is indeed close to B, and one can show that $a \sim b$. The asymptotic (5) is no longer applicable in this case. One should use the asymptotic of the total elliptic integral [8]:

$$K(k) = \frac{\pi}{2}(1+m)[1+\ldots],$$

where $m = (1-k')/(1+k')$, $k' = \sqrt{1-k^2}$.

In this case one can also derive dependences with the structure similar to that of the formula (2) for the parameters of the contact region a and b. We do not cite them. We obtain for the approach of the probe with the specimen due to deformation:

$$h = (FD)^{2/3}\left(\frac{1}{4A}+\frac{1}{4B}\right)^{-1/3}, \tag{8}$$

It also has the structure similar to equations (3) and (6).

Thus, the approximate relations, which allow the direct determination of the values required through the known parameters of the problem, can be also obtained for the case of close A and B values.

Above, we considered the contact deformations in the region of the contact between the probe and the specimen. However, the overall deformation, which determines the underestimate of the AFM-profile height, also includes the contribution of deformations in the region of the contact between the specimen and the substrate (the model describing the situation where the probe presses on the specimen from above is in mind). In this case, one just requires the A and B parameters to determine in a proper way by considering the geometry of the contact between the specimen with the radius R' (which the probe presses on from above) and the flat substrate:

$$A = \frac{1}{2R'},\ B = \frac{1}{2}\left(\frac{1}{R+2R'}\right). \tag{9}$$

The specimen should be considered as a bent cylinder with the bending radius of the surface contacting with the substrate, $R + 2R'$. The analysis of this case does not differ from that undertaken above for the values of A and B determined by the formula (4).

APPLICATION OF THE ALGORITHM DEVELOPED TO THE COMPARATIVE ANALYSIS OF DEFORMATIONS OF SPECIMENS WITH DIFFERENT RADII VALUES

To test the algorithm developed, we used it to calculate contact deformations in the model cases of a cylindrical specimen with the radius of 1 and 10 nm. The results of the numerical calculations are given in Table 1 where the same parameters of the problem are used for the sake of convenience.

The calculations, according to the approximate methods, give the following differences from the exact solution. For $R' = 1$ nm, the approximate solution for different A and B gives a difference of about 2% in the values a and b, and 0.5% in the value of h. For $R' = 10$ nm, the approximate solution for the close A and B gives a difference from the exact solution of about 10% in the values a and b, and 1% in the value of h.

The main conclusion drawn from Table 1 is that the relative deformations of the objects with a smaller curvature radius are essentially higher, providing that the other conditions are the same. Thus, we explained the experimental effect mentioned above and manifesting

Table 1. Comparative analysis of contact deformations in the model of a cylindrical specimen for various radius values.

R'	Contact region	a, b, nm	P, 10^9 Pa	h, nm	ε, %
1 nm	Probe/specimen	0.46; 2.2	1.6	0.36	18
	Specimen/substrate	0.47; 2.4	1.5	0.34	17
	Summary deformation			0.7	35
10 nm	Probe/specimen	1.1; 1.8	0.8	0.29	1.4
	Specimen/substrate	1.3; 2.7	0.4	0.21	1
	Summary deformation			0.5	2.5

Note. The parameters of the problem: the Young modulus of the specimen $E' = 10^{10}$ Pa, and that of the probe $E = 10^{11}$ Pa, the value of the compressing force $F = 5\times10^{-9}$ N, the curvature radius of the probe nib $R = 10$ nm. ε is the relative deformation $(h/2R')\times100\%$.

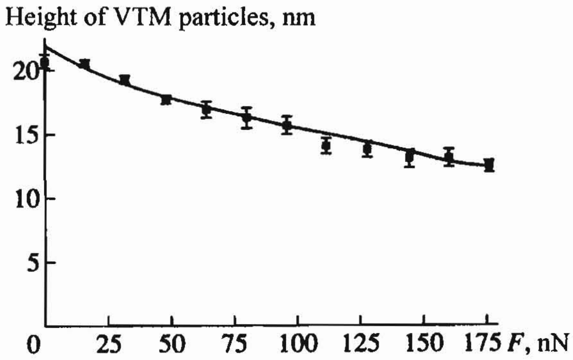

Figure 1. Experimental (points) and theoretical (line) dependences of the deformation of VTM particles on the value of the loading force in the scanning.

itself in the fact that the relative deformations of the nucleic acid molecules substantially exceed the relative deformations of VTM molecules.

COMPARISON WITH THE EXPERIMENTAL DATA

For experimental verification of the "two thirds" law (6), (8)

$$h \sim (FD)^{2/3} f(R, R'), \tag{10}$$

we studied the deformation of VTM particles and DNA molecules using various values of the loading scanning force.

A good agreement between the experiment and the theory (10) was observed for VTM particles (Fig. 1). The experimental errors were determined as a standard deviation of the simple mean in the statistical processing of the values obtained by analyzing several AFM-images for the specific magnitude of the scanning force.

The theoretical dependence was obtained by the method of the analysis of contact deformations of a cylindrical specimen (exact solution) as considered above. The values $R = 25$ nm and $E' = 3\times10^9$ Pa found experimentally were used in the analysis. It follows from Fig. 1 that the "two thirds" law (10) is valid for the case studied in a wide range of forces, except for the region of the minimal efforts. It can be related to the fact that the presence of capillary forces in the experiment in the air does not make it possible to minimize the force of the probe onto the specimen to the value smaller than a few nanonewtons.

The corresponding experimental dependence for DNA molecules is presented in Fig. 2. The experiment was conducted in the same scheme and under the same conditions as in the case of the analysis of VTM deformations. However, in the case considered, the deformations cannot be described by the "two thirds" law (10). Instead, we observe a usual

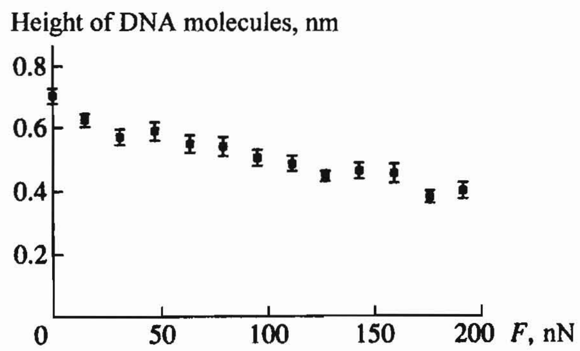

Figure 2. Experimental dependences of the deformation of DNA molecules on the value of the loading force.

linear dependence, i.e., the Hook law. This is explained by the failure of the condition of small deformations, which justifies the conclusions of the contact theory. The fact that the relative deformations measured experimentally for the case of DNA molecules are large even at small forces caused by the probe is explained by the presence of the capillary forces (a capillary bridge). They do not permit one to minimize the scanning force in the air and to provide the values, which are less than a few nanonewtons.

The work was supported by the Russian Foundation for Basic Research, grant no. 97-03-32778a. The authors express their gratitude to Yu. F. Drygin for the preparation of VTM specimens, and to V. V. Prokhorov and D. V. Klinov for kindly supplying them with the DNA specimen.

REFERENCES

1. A. S. Andreeva, M. O. Gallyamov, O. A. Pyshkina, *et al.*, *Zh. Fiz. Khimii*, **73(11)**: 2062 (1999) (in Russian). 2. C. Bustamante, J. Vesenka, C. L. Tang, *et al.*, *Biochemistry*, **31**: 22 (1992).
3. Yu. F. Drygin, O. A. Bordunova, M. O. Gallyamov, and I. V. Yaminsky, *FEBS Letters*, **425**: 217 (1998).
4. M. Yu. Gallyamov, Yu. F. Drygin, and I. V. Yaminsky, *Poverkhnost'*, **7**: 104 (1999) (in Russian).
5. Z. Shao, J. Mou, D. M. Czajkowsky, *et al.*, *Adv. Phys.*, **45(1)**: 1 (1996).
6. H. Herz, *J. Reine Angew. Math.*, **92**: 156 (1882).
7. L. D. Landau and E. M. Lifshitz, *Theory of Elasticity* (Moscow: Nauka) (1987) (in Russian).
8. G. B. Dwait, *Tables of Integrals* (Moscow: Nauka) (1973) (Russian translation).